

Inhomogeneous condensation in the Gross-Neveu model in noninteger spatial dimensions $1 \leq d < 3$

Laurin Pannullo*

*Institut für Theoretische Physik, Goethe-Universität Frankfurt am Main,
Max-von-Laue-Straße 1, D-60438 Frankfurt am Main, Germany.*

(Dated: August 8, 2023)

The Gross-Neveu model in the $N \rightarrow \infty$ limit in $d = 1$ spatial dimensions exhibits a chiral inhomogeneous phase (IP), where the chiral condensate has a spatial dependence that spontaneously breaks translational invariance and the \mathbb{Z}_2 chiral symmetry. This phase is absent in $d = 2$, while in $d = 3$ its existence and extent strongly depends on the regularization and the value of the finite regulator. This work connects these three results smoothly by extending the analysis to noninteger spatial dimensions $1 \leq d < 3$, where the model is fully renormalizable. To this end, we adapt the stability analysis, which probes the stability of the homogeneous ground state under inhomogeneous perturbations, to noninteger spatial dimensions. We find that the IP is present for all $d < 2$ and vanishes exactly at $d = 2$. Moreover, we find no instability towards an IP for $2 \leq d < 3$, which suggests that the IP in $d = 3$ is solely generated by the presence of a regulator.

Keywords: Gross-Neveu model, inhomogeneous phases, moat regime, stability analysis, noninteger spatial dimensions, mean-field

I. INTRODUCTION

A chiral inhomogeneous phase (IP) features a condensate with a spatial dependence that spontaneously breaks translational invariance in addition to chiral symmetry (see Ref. [1] for an extensive review). While phases with inhomogeneous order parameters are well established in condensed matter physics, they are a rather exotic phenomenon in high-energy contexts. In Quantum Chromodynamics (QCD) an IP occurs in the limit of infinite number of colors N_c and at asymptotically large chemical potential [2]. For the physical case of $N_c = 3$, there are also indications for the realization of such a phase at low temperature and high baryon chemical potential as provided by a Dyson-Schwinger equation (DSE) based study that used specific ansatz functions for the inhomogeneous condensate [3]. Recent technical developments [4] might even enable an ansatz-free investigation of the IP within the DSE framework. Moreover, a functional renormalization group study of QCD [5] found a so-called moat regime, where the wave-function renormalization assumes negative values. Such a regime is closely related to the existence of an IP and the implications of such a non-trivial dispersion relation might also be measurable in an experiment [6–9]. Furthermore, it was shown that inhomogeneous ground states can naturally be found in theories with \mathcal{PT} -type symmetries, which is also realized in finite-density QCD [10, 11].

However, due to the lack of first principle calculations of QCD at low temperature and high chemical potential, it is not clear whether the IP is indeed realized in nature or what the extent of the moat regime might be. Therefore, more often IPs are investigated in Four-Fermion (FF) and related Yukawa-models, some of which can be regarded as toy-models for QCD [1]. A prominent example is the $(1+1)$ -dimensional Gross-Neveu (GN) model [12] in the infinite N limit (equivalent to a mean-field approximation in this model), where all quantum fluctuations of the bosonic degrees of freedom are neglected. It features a homogeneously broken phase (HBP) at low temperature and baryon chemical potential, where the constant, nonzero chiral condensate breaks the discrete \mathbb{Z}_2 chiral symmetry that is realized in the model. This phase is separated from a chirally symmetric phase (SP) by a second order line at high temperatures and low chemical potentials that bends down to lower temperatures for increasing chemical potential and ends in a critical point (CP) [13, 14]. If the chiral condensate is restricted to being homogeneous, a first order phase transition extends from this CP down to zero temperature. However, for spatially dependent condensates, the CP coincides with a Lifshitz point (LP) from which an IP opens up to lower temperatures and higher chemical potentials [14–16]. The coincidence of these points is a feature of the GN model (and Nambu-Jona-Lasinio (NJL)-type models) in various dimensions [16–20] that can be broken up by introducing additional vector interactions [21, 22]. These points can also separate as the result of artifacts at finite regulators in certain regularization schemes [18, 20, 23]. In addition, the model also exhibits a moat regime within a region in the phase diagram that is larger than the IP itself [17]. While the phase diagram of the $(1+1)$ -dimensional GN and the related chiral GN model (sometimes also called NJL₂

* pannullo@itp.uni-frankfurt.de

model), which features a continuous chiral symmetry, is fairly understood in the infinite- N limit, it is under intense investigation for finite N . Currently, there is no final consensus about which phases persist with full bosonic quantum fluctuations [24–31]. However, recent work [31] showed that the feature of negative wave-function renormalization and moat regimes at large μ is robust under the influence of bosonic fluctuations.

In contrast to the infinite N results in $1 + 1$ dimensions stands the phase diagram of the same GN model in $2 + 1$ dimensions, where no IP for any chemical potential and nonzero temperature is present [23, 32–34]. One only finds a second order line separating the HBP at low temperature and chemical potential from the SP, which ends in a CP at zero temperature [35, 36]. It was found that keeping regulators such as the lattice spacing or the Pauli-Villars mass at a finite value, causes the CP to be located at a nonzero temperature and the emergence of an IP [23]. An extended analysis in $2 + 1$ dimensions revealed that a large class of FF models featuring Lorentz-(pseudo)scalar interactions and their Yukawa model extensions do not exhibit an IP [34]. Thus, the absence of an IP in the $(2 + 1)$ -dimensional GN model is apparently part of a more general behavior of FF models in $2 + 1$ dimensions. Still it is not clear what the cause of the absence of the IP compared to $1 + 1$ dimensions is. There has also been considerable effort in understanding the phase structure of the $(2 + 1)$ -dimensional GN model beyond the infinite- N limit for finite temperature, chemical potential and magnetic field with lattice and functional methods (see e.g. [37–44]). However, there is no concrete evidence for inhomogeneous condensation for finite N .

In $3 + 1$ dimensions, the GN and NJL model exhibit an identical phase diagram in the chiral limit within the mean-field approximation [19]. In general, one finds a similar phase structure as for the GN model in $d = 1$ with all three phases and a CP present. These models are, however, non-renormalizable in $d = 3$ and thus one has to keep the employed regulator (e.g. the Pauli-Villars mass) at a finite value. The phase structure of the theory is strongly dependent on the chosen regularization scheme and value of the regulator [45–48]. Varying these can lead to a disappearance of the CP for the homogeneous phase transition [46], a splitting of LP and CP [18, 19, 23, 49], and an absence of the IP altogether [45, 47].

In this work, we connect these three results from integer dimensions and illustrate why the model shows these qualitatively different phase diagrams. To this end, we consider the GN model in the mean-field approximation in noninteger number of spatial dimensions $1 \leq d < 3$. This builds on the results of Ref. [50] where the dependence of the homogeneous phase diagram on d was investigated. We extend this by an investigation of the IP and the moat regime based on the bosonic two-point function.

The so-called stability analysis, which probes the stability of a homogeneous field configuration against spatially inhomogeneous perturbations by inspection of the bosonic two-point functions, is a common technique to study IPs. This method was already used to investigate the IP in integer spatial dimensions $d = 1, 2, 3$ within the GN and related models (see, e.g., Refs. [17, 23, 47, 51–56]) and we extend this technique to noninteger spatial dimensions $1 \leq d < 3$. The model is renormalizable for $1 \leq d < 3$ and the analysis can be formulated independently from details like the fermion representation. Thus, in this setup the only parameter left is the number of spatial dimensions, which allows us to study its influence isolated from other effects. At this point it needs to be noted that the concept of noninteger spatial dimensions is something peculiar – especially since we are investigating a spatial phenomenon. Therefore, we should consider the number of spatial dimensions d merely as a parameter that we can vary to interpolate between the physically relevant integer dimensions. The study is restricted to zero temperature as it suffices to demonstrate the central findings and makes it possible to give closed form expression for most of the derived quantities.

We find that the instability towards the IP gradually disappears when going from $d = 1$ to $d = 2$. Since this setup depends only on d as a parameter, we can identify the number of spatial dimensions as the sole cause of the disappearance of the IP in $d = 2$. Furthermore, there is no instability for $2 < d < 3$, which suggests that the presence of an IP in studies of $(3 + 1)$ -dimensional models is caused by the presence of finite regulators.

This paper is structured as follows. Section II introduces the GN model in d spatial dimensions. The homogeneous effective potential at zero temperature and aspects of the homogeneous phase transition are discussed in Section II A. The key quantities of the stability analysis are introduced in Section II B and the main results of the stability analysis are presented in Section III, which is split between spatial dimensions $1 \leq d \leq 2$ and $2 \leq d < 3$. Section IV provides a brief conclusion and outlook on future extensions to this work. The Appendices A and B present technical aspects of the derivation of the effective potential, the stability analysis and the wave-function renormalization.

II. THE GROSS-NEVEU MODEL IN $1 \leq d < 3$ SPATIAL DIMENSIONS

We consider the action of the GN model in $D = d + 1$ spacetime dimensions

$$\mathcal{S}[\bar{\psi}, \psi] = \int_0^\beta d\tau \int d^d x \left[\bar{\psi}(\not{\partial} + \gamma_0 \mu)\psi - \frac{\lambda}{2N} (\bar{\psi}\psi)^2 \right], \quad (1)$$

where ψ are fermionic spinors with $N \times N_\gamma$ degrees of freedom (number of flavors¹ \times dimension of the representation of the Clifford algebra). The Euclidean time direction, i.e., the zeroth direction, is compactified with its extent β corresponding to the inverse temperature $\beta = 1/T$ and the d -dimensional spatial integration goes over the d -dimensional volume V . In the actual calculations, we will assume both V and β to be infinite and hence consider the theory at zero temperature in an infinite volume. A baryon chemical potential μ is introduced in the standard way and the coupling λ controls the strength of the FF interaction.

By applying a Hubbard-Stratonovich transformation, we remove the FF interaction and introduce a real, scalar bosonic field σ in the action

$$\mathcal{S}_\sigma[\bar{\psi}, \psi, \sigma] = \int_0^\beta d\tau \int d^d x \left[\frac{N}{2\lambda} \sigma^2 + \bar{\psi}(\not{\partial} + \gamma_0 \mu + \sigma)\psi \right], \quad (2)$$

where the introduced bosonic field fulfills the Ward identity

$$\langle \bar{\psi}(x)\psi(x) \rangle = \frac{-N}{\lambda} \langle \sigma(x) \rangle \quad (3)$$

that connects the expectation values of the chiral condensate and the bosonic field at the spacetime point x . The model possesses a discrete \mathbb{Z}_2 chiral symmetry in integer dimensions under the transformation

$$\psi \rightarrow \gamma_5 \psi, \quad \bar{\psi} \rightarrow -\bar{\psi} \gamma_5, \quad \sigma \rightarrow -\sigma, \quad (4)$$

where γ_5 is the Dirac matrix that anti-commutes with the spacetime Dirac matrices. Thus, the auxiliary field σ also serves as an order parameter of the spontaneous breaking of the chiral symmetry. The special connection between chirality and the number of spacetime dimensions, as well as the ambiguities of defining γ_5 [57] in noninteger dimensions cause the chiral symmetry to be strictly present only in integer dimensions. Nevertheless, in analogy to this symmetry, we denote phases with $\langle \sigma \rangle \neq 0$ as HBP (or IP, if $\langle \sigma \rangle$ is spatially dependent) as well as phases with $\langle \sigma \rangle = 0$ as SP even in noninteger dimensions.

Moreover, one has to choose a reducible representation of the Clifford algebra in odd spacetime dimensions in order to find an additional matrix that anti-commutes with the spacetime Dirac matrices. This is particularly relevant in 2+1 dimensions, where one needs to use a reducible 4×4 representation to regain the notion of chirality [23, 51, 58, 59]. Even though our analysis will be independent of specific representations and their dimensions, we will assume a representation that enables the existence of a matrix γ_5 in the respective integer dimensions. Irrespective of the number of dimensions and representation, we can assume the standard anti-commutation relation for the spacetime Dirac matrices $\{\gamma_\mu, \gamma_\nu\} = 2\delta_{\mu\nu}\mathbf{1}$ to hold [57].

Integrating over the fermionic fields in the path integral yields the so-called effective action

$$\frac{\mathcal{S}_{\text{eff}}[\sigma]}{N} = \int_0^\beta d\tau \int d^d x \frac{\sigma^2}{2\lambda} - \ln \text{Det} [\beta (\not{\partial} + \gamma_0 \mu + \sigma)], \quad (5)$$

where Det denotes a functional determinant. In the following, we consider only the leading term in a $1/N$ expansion (equivalent to a mean-field approximation in this case), which neglects all quantum fluctuations of σ . Then, the only field configurations Σ that contribute to the path integral are these that minimize the effective action \mathcal{S}_{eff} globally. In the case of a broken symmetry, there are multiple such field configurations which are connected by the transformations of the broken symmetry. One typically picks one of these configurations in the evaluation of observables (compare, e.g., Refs. [17, 19]). This is equivalent to introducing an explicit breaking to the action and extrapolating this term to zero.

The model is renormalizable for $d < 3$ [60] and we use as a renormalization condition that the vacuum expectation value of the auxiliary field assumes a finite homogeneous value $\langle \sigma \rangle|_{T=\mu=0} = \bar{\sigma}_0$. The UV-divergent contributions from loop integrals are regularized with a spatial momentum cutoff. This regularization scheme is chosen due to its simplicity and its application being independent of the number of spatial dimensions. The scheme restricts the spatial loop momenta to a d -dimensional sphere with radius Λ in the regularized integrals and Λ is then sent to infinity in the renormalization procedure.

¹ Note that within the GN model, “flavors” is the traditional name for this degree of freedom in which the interactions are diagonal. Hence, these flavors are distinctively different from an isospin degree of freedom or quark flavors in QCD.

A. The homogeneous effective potential at zero temperature

We define the homogeneous effective potential \bar{U}_{eff} as the effective action of the homogeneous bosonic field per volume and degree of freedom, i.e.,

$$\bar{U}_{\text{eff}}(\bar{\sigma}, \mu, d) := \frac{\mathcal{S}_{\text{eff}}[\bar{\sigma}]}{NV\beta}, \quad (6)$$

where $\bar{\sigma}$ is the bosonic field restricted to homogeneous field configurations, i.e., $\bar{\sigma} = \text{const.}$ We proceed to calculate the homogeneous effective potential at zero temperature in the infinite spatial volume

$$\begin{aligned} \bar{U}_{\text{eff}}(\bar{\sigma}, \mu, d) &= \frac{\bar{\sigma}^2}{2\lambda} - \frac{1}{\beta V} \ln \text{Det}(\not{\partial} + \gamma_0 \mu + \bar{\sigma}) = \\ &= \frac{\bar{\sigma}^2}{2\lambda} - \frac{N_\gamma}{2} \int \frac{d^d p}{(2\pi)^d} [E - \Theta(\mu^2 - E^2)(E - |\mu|)] = \\ &= \frac{\bar{\sigma}^2}{2\lambda} - \frac{N_\gamma}{2} l_0(\bar{\sigma}^2, \mu), \end{aligned} \quad (7)$$

where $E^2 = \bar{\sigma}^2 + \mathbf{p}^2$. The integral l_0 is obviously UV-divergent for every number of spatial dimensions $d > 0$. We renormalize the effective potential with the condition $\langle \sigma \rangle|_{T=\mu=0} = \bar{\sigma}_0$ (see Section II). This condition corresponds to $\min_{\bar{\sigma}} \bar{U}_{\text{eff}}|_{T=\mu=0} = \bar{\Sigma}|_{T=\mu=0} = \bar{\sigma}_0$ within the infinite N limit. Therefore, $\bar{\sigma}_0$ fulfills the homogeneous gap equation

$$\begin{aligned} \left. \frac{d\bar{U}_{\text{eff}}}{d\bar{\sigma}} \right|_{T=\mu=0, \bar{\sigma}=\bar{\sigma}_0} &= \left[\frac{\bar{\sigma}}{\lambda} - \bar{\sigma} N_\gamma \int_{-\infty}^{\infty} \frac{dp_0}{(2\pi)} \int_{\Lambda} \frac{d^d p}{(2\pi)^d} \frac{1}{(p_0 - i\mu)^2 + E^2} \right] \Bigg|_{T=\mu=0, \bar{\sigma}=\bar{\sigma}_0} = \\ &= \left[\bar{\sigma} \left(\frac{1}{\lambda} - N_\gamma l_1 \right) \right] \Bigg|_{T=\mu=0, \bar{\sigma}=\bar{\sigma}_0} \stackrel{!}{=} 0, \end{aligned} \quad (8)$$

which is used to tune the coupling λ in order to renormalize the theory.

Appendix A outlines the calculation of l_0 and l_1 for spatial dimensions $1 \leq d < 3$, which are needed to obtain the renormalized effective potential

$$\begin{aligned} \bar{U}_{\text{eff}}(\bar{\sigma}, \mu, d) &= \frac{N_\gamma}{2^d \pi^{\frac{d}{2}}} \left[\frac{(d+1)\Gamma(-\frac{d+1}{2})}{8\sqrt{\pi}} \left(-\frac{\bar{\sigma}_0^{d-1} \bar{\sigma}^2}{2} + \frac{|\bar{\sigma}|^{d+1}}{d+1} \right) + \right. \\ &\quad \left. + \frac{\Theta(\bar{\mu}^2)}{d\Gamma(\frac{d}{2})} |\bar{\sigma}|^{d+1} \left| \frac{\bar{\mu}}{\bar{\sigma}} \right|^d \left({}_2F_1\left(-\frac{1}{2}, \frac{d}{2}; \frac{d+2}{2}; -\frac{\bar{\mu}^2}{\bar{\sigma}^2}\right) - \left| \frac{\mu}{\bar{\sigma}} \right| \right) \right], \end{aligned} \quad (9)$$

where ${}_2F_1$ is the Gaussian hypergeometric Function defined by Eq. (A2), $\bar{\mu}^2 = \mu^2 - \bar{\sigma}^2$ and a divergent, thermodynamically irrelevant constant term is neglected. The effective potential in noninteger spatial dimensions was first investigated in Ref. [50]. However, a closed form expression for $T = 0$ and finite chemical potential was not explicitly given and thus we provide it for completeness.

For homogeneous fields, one finds by inspection of \bar{U}_{eff} for all number of spatial dimensions $1 \leq d < 3$ an HBP at low chemical potential indicated by the minimizing field value $\bar{\Sigma}$ being nonzero. For chemical potentials larger than a critical chemical potential $\mu_c(d)$, the system enters the SP signaled by $|\bar{\Sigma}| = 0$ (see Ref. [50] for a detailed discussion of the homogeneous phase structure). Figure 1 shows the renormalized effective potential $\bar{U}'_{\text{eff}}(\bar{\sigma}, \mu_c(d), d) = \bar{U}_{\text{eff}}(\bar{\sigma}, \mu_c(d), d) - \bar{U}_{\text{eff}}(0, \mu_c(d), d)$ ² in the $\bar{\sigma}, d$ -plane at the critical chemical potential $\mu_c(d)$ with the red dashed lines indicating the minima $\bar{\Sigma}(d)$. This illustrates how the phase transition is of first order for $d < 2$ due to the potential barrier separating the two minima at $\bar{\Sigma} = 0, \bar{\sigma}_0$. The potential is flat for $|\bar{\sigma}| \leq \bar{\sigma}_0$ at $d = 2$, which is caused by a combined effect of zero temperature and the CP being located at this point. Ref. [50] documents how this CP evolves from $(\mu, T)/\bar{\sigma}_0 \approx (0.608, 0.318)$ in $d = 1$ to $(\mu, T)/\bar{\sigma}_0 = (1.0, 0)$ in $d = 2$. For $d > 2$ the CP vanishes and the homogeneous phase transition is strictly of second order.

² The symmetric contribution is subtracted in order to facilitate the comparison between different d .

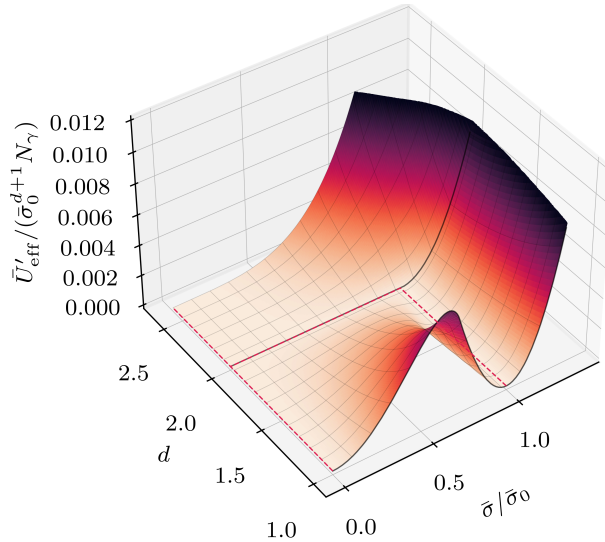


FIG. 1. The renormalized effective potential $\bar{U}'_{\text{eff}}(\bar{\sigma}, \mu_c(d), d) = \bar{U}_{\text{eff}}(\bar{\sigma}, \mu_c(d), d) - \bar{U}_{\text{eff}}(0, \mu_c(d), d)$ in the $\bar{\sigma}, d$ -plane at the critical chemical potential $\mu_c(d)$, where the homogeneous phase transition occurs. The red dashed lines indicate the minima $\bar{\Sigma}(d)$.

B. Stability analysis at zero temperature

The key concept of the stability analysis is to apply an arbitrary inhomogeneous perturbation of infinitesimal amplitude to a homogeneous field configuration $\bar{\sigma}$ and analyze the curvature of the effective action \mathcal{S}_{eff} under this perturbation. If the global homogeneous minimum $\bar{\Sigma}$ is used as an expansion point, a negative curvature indicates that there exists an inhomogeneous field configuration with an even lower action and thus confirms the existence of an IP. For a detailed derivation of the stability analysis in the GN model in 1 + 1 and 2 + 1 dimensions we refer to Refs. [17, 23]. Here, we present only the final result for the bosonic two-point function $\Gamma^{(2)}$, which is the previously mentioned curvature of the effective action in the direction of an inhomogeneous perturbation of momentum \mathbf{q} to the homogeneous bosonic field $\bar{\sigma}$. One finds that this curvature is only dependent on the magnitude of the bosonic momentum $|\mathbf{q}| = q$ and not its direction in the d -dimensional space. This circumstance makes it possible to apply this technique in noninteger spatial dimensions.

The two-point function at zero temperature has the general form

$$\Gamma^{(2)}(\bar{\sigma}^2, \mu, q^2, d) = \frac{1}{\lambda} - N_\gamma l_1(\bar{\sigma}^2, \mu, d) + L_2(\bar{\sigma}^2, \mu, q^2, d), \quad (10)$$

where we recognize the same contribution $1/\lambda - N_\gamma l_1$ as in the gap equation and that the whole momentum dependence resides in L_2 , which is given by

$$L_2(\bar{\sigma}^2, \mu, q^2, d) = \frac{1}{2} (q^2 + 4\bar{\sigma}^2) N_\gamma \int_{-\infty}^{\infty} \frac{dp_0}{(2\pi)} \int \frac{d^d p}{(2\pi)^d} \frac{1}{((p_0 - i\mu)^2 + \bar{\sigma}^2 + (\mathbf{p} + \mathbf{q})^2)((p_0 - i\mu)^2 + \bar{\sigma}^2 + \mathbf{p}^2)}. \quad (11)$$

The evaluation of this expression for arbitrary $1 \leq d < 3$ is outlined in Appendix B, while for the integer cases of $d = 1$ we refer to Ref. [17] and for $d = 2$ to Ref. [23]. We find for arbitrary spatial dimensions $1 \leq d < 3$ that the two-point function evaluates to

$$\Gamma^{(2)}(\bar{\sigma}^2, \mu, q^2, d) = \frac{N_\gamma}{2^d \pi^{\frac{d}{2}} \Gamma(\frac{d}{2})} \left[\frac{\Gamma(\frac{1-d}{2}) \Gamma(\frac{d+2}{2})}{d\pi} (|\bar{\sigma}_0|^{d-1} - |\bar{\sigma}|^{d-1}) + \right. \quad (12)$$

$$\left. + \begin{cases} \frac{|\mu|^{d-1}}{(d-1)} & \text{if } \bar{\sigma} = 0, \mu \neq 0 \\ \frac{|\bar{\sigma}|^{d-1}}{d} \left| \frac{\bar{\mu}}{\bar{\sigma}} \right|^d {}_2F_1\left(\frac{1}{2}, \frac{d}{2}; \frac{d+2}{2}; -\frac{\bar{\mu}^2}{\bar{\sigma}^2}\right) & \text{if } \bar{\sigma} \neq 0, \bar{\mu}^2 > 0 \\ 0 & \text{otherwise} \end{cases} \right]$$

$$+ \left(\frac{q^2}{4} + \bar{\sigma}^2 \right) \int_0^1 dx \times \left\{ \begin{array}{ll} \frac{\tilde{\mu}^{d-3}}{(3-d)} {}_2F_1 \left(\frac{3}{2}, \frac{3-d}{2}; \frac{3-d}{2} + 1; -\frac{\tilde{\Delta}^2}{\tilde{\mu}^2} \right) - \frac{\tilde{\mu}^{d-2}}{|\mu|} & \text{if } \tilde{\mu}^2 > 0 \\ \frac{\tilde{\Delta}^{d-3}}{2} B \left(\frac{d}{2}, \frac{3-d}{2} \right) & \text{otherwise} \end{array} \right\},$$

where $\tilde{\Delta}^2 = \bar{\sigma}^2 + q^2 x(1-x)$ and $\tilde{\mu}^2 = \mu^2 - \tilde{\Delta}^2$. The remaining integral over x is evaluated numerically since no closed form can be given for the integral.

The other quantity of interest is the bosonic wave-function renormalization z , where negative values indicate a moat regime. This z is the coefficient of the bosonic kinetic term $\propto 1/2 \partial_\mu \sigma \partial_\mu \sigma$ in the effective action that is contained in the fermionic contribution³. We can calculate z from the bosonic two-point function by differentiating it twice with respect to q and setting $q = 0$ [17], i.e.,

$$z(\bar{\sigma}, \mu, d) = \frac{1}{2} \frac{d^2 \Gamma^{(2)}(\bar{\sigma}, \mu, q^2, d)}{dq^2} \Big|_{q=0} = \frac{N_\gamma}{2^{d+2} \pi^{\frac{d}{2}} \Gamma(\frac{d}{2})} \times \left\{ \begin{array}{ll} \frac{1}{(3-d)\tilde{\mu}^{3-d}} {}_2F_1 \left(\frac{3}{2}, \frac{3-d}{2}; \frac{5-d}{2}; -\frac{\bar{\sigma}^2}{\tilde{\mu}^2} \right) + \\ - \frac{1}{(5-d)} \frac{\bar{\sigma}^2}{\tilde{\mu}^2} \frac{1}{\tilde{\mu}^{3-d}} {}_2F_1 \left(\frac{5}{2}, \frac{5-d}{2}; \frac{7-d}{2}; -\frac{\bar{\sigma}^2}{\tilde{\mu}^2} \right) + \\ + \frac{\tilde{\mu}^{d-2}}{|\mu|} \left[\frac{\bar{\sigma}^2}{\mu^2} \left(1 + \frac{1}{3\tilde{\mu}^2} (2\bar{\sigma}^2 - (4-d)\mu^2) \right) - 1 \right] & \text{if } \tilde{\mu}^2 > 0 \\ \frac{1}{2|\bar{\sigma}|^{3-d}} [B(\frac{d}{2}, \frac{3-d}{2}) - B(\frac{d}{2}, \frac{5-d}{2})] & \text{otherwise} \end{array} \right. \quad (13)$$

The derivation of z is outlined in Appendix B. If z is evaluated on the global homogeneous minimum $\bar{\Sigma}(\mu, d)$, we denote it as $Z(\mu, d) \equiv z(\bar{\Sigma}(\mu, d), \mu, d)$.

III. RESULTS OF THE STABILITY ANALYSIS

In this section the results that are obtained by the stability analysis of the GN model for $1 \leq d < 3$ spatial dimensions are discussed. The discussion is split in $1 \leq d \leq 2$ and $2 \leq d < 3$ due to the different conclusions that we can draw from these two intervals.

A. $1 \leq d \leq 2$

Figure 2 shows the two-point functions $\Gamma^{(2)}(\bar{\Sigma}^2, \mu_c^+, q^2, d)$ for $1 \leq d \leq 2$ spatial dimensions at $\mu = \mu_c^+$, which is the critical chemical potential with an infinitesimal positive shift. This ensures that the homogeneous minimum used as the expansion point is $\bar{\Sigma} = 0$. For $d = 1$, the two-point function diverges logarithmically at $q = 2\mu$ for all $\mu > \mu_c$ as also observed in Ref. [17]. For $1 < d < 2$, the integral over x in Eq. (12) has to be performed numerically. It is thus not immediately clear, whether the two-point function diverges as in $d = 1$ for $q = 2\mu$. The integrand in Eq. (12) is divergent at $x = 1/2$ for $\bar{\sigma} = 0, q = 2\mu$ and expanding it at $x_0 = 1/2$ reveals that the most divergent term is $\propto (x - 1/2)^{d-2}$. Hence, the integral over x is finite for any $d > 1$. Thus, the divergence of the two-point functions vanishes for $d > 1$, but a cusp that is a negative minimum is retained. This preserves the instability at μ_c for $1 < d < 2$. However, one finds that the offset of $\Gamma^{(2)}$ at $q = 0$ increases with increasing μ . Thus, for $1 < d < 2$ there is an upper μ at which the IP vanishes (see Fig. 6).

It was documented in Ref. [17] that in the (1+1)-dimensional GN model there is a region of the IP in the μ - T -plane that is not detected by the stability analysis. This is where the homogeneous minimum $\bar{\Sigma}$ assumes a finite value, which is separated from the true inhomogeneous minimum by an energy barrier. Thus, $\bar{\Sigma}$ appears to be stable against inhomogeneous perturbations even though an inhomogeneous condensate is energetically preferred [14]. We expect this to happen in some portion of the phase diagram for all spatial dimensions $1 < d < 2$, since the first order phase transition, which was identified as the cause of this effect in $d = 1$, is also present there.

³ This term can be explicitly seen in an expansion of the $\ln \text{Det}$ contribution in the effective action (5), e.g., in a Ginzburg-Landau approach. See also Ref. [31] for a study of Z in the (1+1)-dimensional GN model at finite N , i.e., in the presence of bosonic fluctuations.

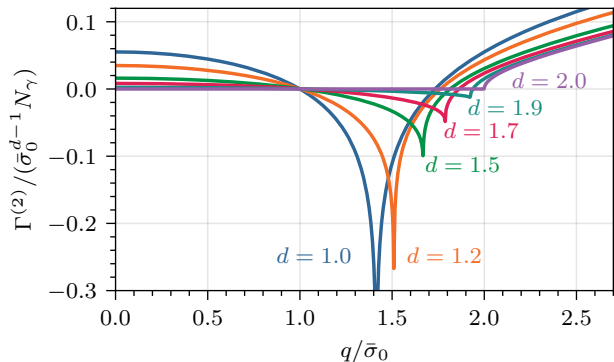


FIG. 2. The two-point function $\Gamma^{(2)}(\bar{\Sigma}^2 = 0, \mu_c^+, q^2, d)$ as a function of the bosonic momentum q for various spatial dimensions $1 \leq d \leq 2$ evaluated at the homogeneous minimum $\bar{\Sigma}$ at chemical potential $\mu = \mu_c^+$ (the critical chemical potential with an infinitesimal positive shift). Compare to Ref. [17] for $d = 1$ and Refs. [23, 34] for $d = 2$.

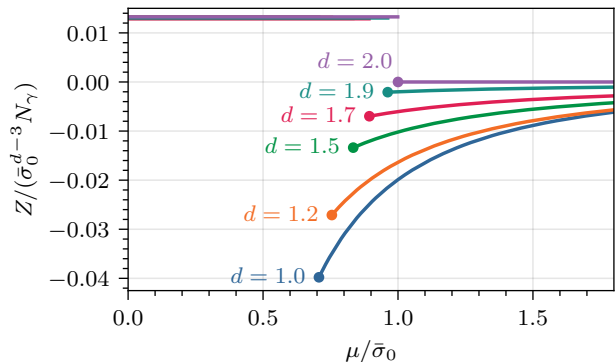


FIG. 3. The wave-function renormalization Z as a function of the chemical potential for various spatial dimensions $1 \leq d \leq 2$. The circle indicates the chemical potential μ_c at which the homogeneous phase transition is located. Compare to Ref. [17] for $d = 1$.

By increasing d further to $d = 2$, the two-point function evolves to the known (2+1)-dimensional result [23, 34]. The two-point function is constant and zero for all $q \leq 2\mu$ at which it rises for $q > 2\mu$. This corresponds to a degeneracy of the homogeneous minimum and field configurations with small inhomogeneous perturbations of momentum $q \leq 2\mu$. Hence, it cannot provide any information about the energetically preferred state. However, it was found that the crystal kink solutions of the (1+1)-dimensional GN model embedded in 2 spatial dimensions are energetically degenerate to homogeneous field configurations even for finite amplitudes at $(\mu, T) = (\mu_c, 0)$ in the (2+1)-dimensional GN model [32].⁴ This observation and our results for the two-point function suggest a flat effective potential for a variety of inhomogeneous modulations. This would be similar to the flat homogeneous potential shown in Fig. 1, which is caused by the special nature of the CP at this point.

We observe that all numbers of spatial dimensions $1 \leq d < 2$, where the CP is also located at a nonzero temperature (as discussed in Section II A), exhibit an instability. This is due to the coincidence of the CP and the LP for the renormalized GN model.

Figure 3 shows the wave-function renormalization evaluated at $\bar{\Sigma}$ as a function of μ for $1 \leq d \leq 2$. We observe $Z < 0$ for $\mu > \mu_c$ and $d < 2$, which is the key property of a moat regime [6–9]. Thus, a moat regime is retained for all chemical potentials for $d < 2$.

B. $2 \leq d < 3$

Figure 4 shows $\Gamma^{(2)}(\bar{\Sigma}^2, \mu, q^2, d)$ for spatial dimensions $2 \leq d < 3$ at $\mu = \mu_c^+$. For spatial dimensions $d > 2$, the constant behavior vanishes and the two-point function approaches a parabolic shape, but the cusp at $q = 2\mu$ remains a non-analytic point. Thus, by inspection of the two-point function we recognize that there is no instability for $2 < d < 3$. This is in stark contrast to existing results of the NJL model in 3+1 dimensions, which exhibits the same phase diagram as the (3+1)-dimensional GN model within the mean-field approximation [19, 50]. Here one finds instabilities towards an IP [47, 52, 61] and even the energetically preferred inhomogeneous condensates by minimizing the effective action with a suitable ansatz [19, 45, 53, 61–65]. Due to the smooth evolution of the two-point function for $1 \leq d < 3$, we would not expect a significant change in behavior caused by increasing the number of dimensions when going from $d < 3$ to $d = 3$. The difference, however, is that while we investigated the renormalized model in $d < 3$, it loses its renormalizability in $d = 3$. Thus, the aforementioned investigations are performed at a finite regulator. It was shown that varying the regularization scheme (e.g. Pauli-Villars regularization, spatial momentum cutoff, lattice regularization) and the value of its regulator can have a severe impact on the existence and extent of the IP [45, 47]. Moreover, the CP coincides with the LP only for some regularization schemes, e.g., Pauli-Villars

⁴ It might be interesting to embed the solutions of the (1+1)-dimensional GN model in $1 < d < 2$ similar to what was done for $d = 2$ in [32]. In this way, one could observe how the degeneracy between homogeneous configurations and these inhomogeneous modulations develops at $d = 2$.

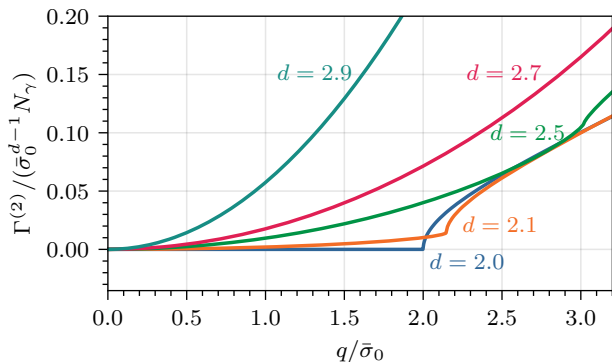


FIG. 4. The two-point function $\Gamma^{(2)}(\bar{\Sigma}^2 = 0, \mu_c^+, q^2, d)$ as a function of the bosonic momentum q for various spatial dimensions $2 \leq d < 3$ evaluated at the homogeneous minimum $\bar{\Sigma}$ at chemical potential $\mu = \mu_c^+$ (the critical chemical potential with an infinitesimal positive shift). Compare to Refs. [23, 34] for $d = 2$.

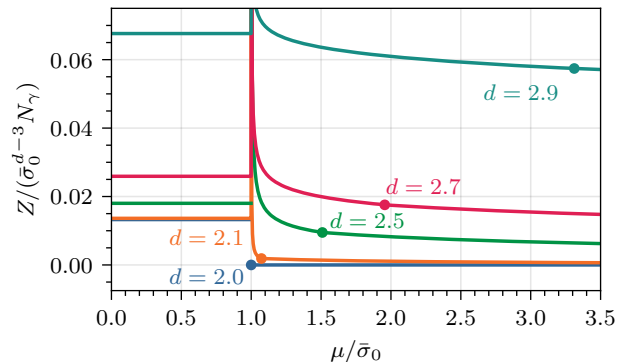


FIG. 5. The wave-function renormalization Z as a function of the chemical potential for various spatial dimensions $2 \leq d < 3$. The circle indicates the chemical potential μ_c at which the homogeneous phase transition is located.

or dimensional regularization. For small enough regulators this CP and with it also the LP is located at a nonzero temperature, which enables the existence of the IP. In a similar fashion an investigation of the $(2+1)$ -dimensional GN model revealed that an IP exists at a finite regulator and vanishes when removing the regulator [23, 33, 51]. This finding and the lack of instability for $2 < d < 3$ in the renormalized setup as presented in this work suggest the conclusion that the existence of the IP in the $(3+1)$ -dimensional GN model (and due to their equivalence also the NJL model) is solely triggered by the choice of the regularization scheme and the presence of a finite regulator.

Figure 5 depicts the bosonic wave-function renormalization Z as a function of the chemical potential for various spatial dimensions $2 \leq d < 3$. While the minimum value of the wave-function renormalization at $d = 2$ is $Z = 0$, it is strictly positive for $2 < d < 3$. Therefore, no moat regime is retained for $d > 2$. Moreover, we note that Z diverges at $\mu/\bar{\sigma}_0 = 1$. This is caused in $2 < d < 3$ by the second order homogeneous phase transition, where the condensate starts to “melt” for chemical potentials $\mu/\bar{\sigma}_0 > 1$. This enables $1 = \mu^2 \approx \bar{\Sigma}(\mu)^2$, which causes divergences in Z (compare to Eq. (13)). Graphically speaking, this is caused by the cusp that is present in the two-point function at $|q| = 2\sqrt{\mu^2 - \bar{\sigma}^2}$, being located at $q = 0$ for $\mu^2 = \bar{\Sigma}^2$. Then, this causes Z , which is the second derivative of the two-point function, to diverge.

IV. CONCLUSION AND OUTLOOK

A. Conclusion

Within the stability analysis one applies inhomogeneous perturbations to the homogeneous ground state and inspects the curvature of the effective action for these perturbations. If one finds negative values for this curvature, which are given by negatives values in the momentum dependence of the bosonic two-point function, the homogeneous field configuration is unstable and an inhomogeneous ground state is energetically preferred.

We adapted this method to noninteger spatial dimensions and illuminated how the instability towards an inhomogeneous phase (IP) in $1+1$ dimensions turns into an absence of instability in $2+1$ dimensions. By continuously increasing the number of spatial dimensions from $d = 1$ to $d = 2$, we observed how the two-point function evolves as a function of d . The IP is present for all $d < 2$ in some range of μ and the instability vanishes exactly at $d = 2$. Moreover, for $1 < d < 2$ there is an upper chemical potential at which the instability vanishes, but a moat regime is retained for all chemical potentials. This renormalized setup is independent of regulators and details like the fermion representation, which allows us to study the isolated effect of the number of dimension. Thus, we identified that the sole driver of the disappearance of the IP at $d = 2$ is the number of spatial dimensions, and by extension the dependence of the critical point (CP) and Lifshitz point (LP) on d .

For $2 < d < 3$, one finds that the two-point function is positive for all bosonic momenta $q \geq 0$ and thus there is no instability towards an IP. This is qualitatively different from existing results in $d = 3$ that exhibit an IP [19, 45, 47, 52, 53, 61–65]. The difference is the need for a finite regulator in $d = 3$ spatial dimensions that can cause

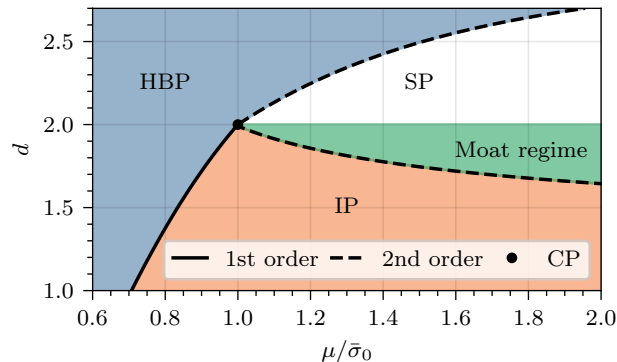


FIG. 6. The phase diagram of the renormalized GN model as obtained from the stability analysis in the plane of spatial dimensions d and chemical potential μ . The phase diagram shows a homogeneously broken phase (HBP) with $\sigma(x) = \bar{\sigma} = \text{const}$, a symmetric phase (SP) with $\sigma(x) = 0$, an inhomogeneous phase (IP) with $\sigma(x) = f(x)$ and a moat regime with negative wavefunction renormalization, i.e., $Z < 0$. The boundaries of the HBP are calculated by Eq. (3.33) and Eq. (3.35) from Ref. [50].

the appearance of a CP and LP at a nonzero temperature. This effect was also observed in the Gross-Neveu (GN) model for $d = 2$ where it led to the appearance of the IP even though it is not present when the model is renormalized [23, 33, 51]. This observation and our results suggest that the appearance of the IP in the $(3 + 1)$ -dimensional GN and Nambu-Jona-Lasinio (NJL) model is generated by the necessary use of a finite regulator.

Figure 6 summarizes these findings in the phase diagram of the renormalized GN model at zero temperature in the plane of the number of spatial dimensions d and chemical potential μ .

Interestingly there is a connection of this work with investigations of the $(3 + 1)$ -dimensional NJL model that use dimensional regularization to regulate the theory [46, 66–69]. Due to the nonrenormalizability of the model, the number of spatial dimensions d has to be fixed at a value $d < 3$ and additionally one has to introduce a mass scale M_0 (because the regulator d itself is dimensionless). Both d and M_0 are then tuned such that certain observables in the vacuum assume fixed values (e.g. the pion decay constant). In this way, one could interpret the present work as the $(3 + 1)$ -dimensional GN model with dimensional regularization, since the applied renormalization also introduced a mass scale $\bar{\sigma}_0$ and we vary the dimensions d . In this picture, by analyzing the phase structure for different d , we really investigate the regulator dependence of the phase diagram of the $(3 + 1)$ -dimensional GN model for the dimensional regularization scheme. Vice versa, the effect of considering $(3 + 1)$ -dimensional models with dimensional regularization at finite regulator is that one generates the phase structure of lower dimensional versions of the respective models.

B. Outlook

An obvious extension of the present work might be the investigation of the NJL model. It features an additional Yukawa interaction term with a pion field of the form $\bar{\psi}i\gamma_5\vec{\tau}\cdot\vec{\pi}\psi$. However, the ambiguities of γ_5 in noninteger dimensions lead to an altered anti-commutation relation $\{\gamma_\mu, \gamma_5\}$ [57], which significantly changes the renormalization and the stability analysis of the NJL model compared to integer dimensions. While it is still possible to conduct the stability analysis, the results depend on these ambiguities in noninteger dimensions and thus no results for this model are presented. A more detailed discussion of the resulting implications can be found in Ref. [70].

Most investigations of the IP in $(3 + 1)$ -dimensional models (see, e.g., Refs. [18, 19, 21, 22, 49, 52, 63, 64]) use the Pauli-Villars regularization. In order to connect better to these results, it would be instructive to carry out the present analysis in noninteger spatial dimensions with the Pauli-Villars regularization at a finite regulator. In this way, one could show that it is possible to regain an IP for $2 < d \leq 3$ by considering appropriate values of the regulator and smoothly connect our noninteger analysis to established, finite regulator results in $d = 3$.

Several investigations in integer dimensions (e.g. Refs. [19, 32]) have embedded 1-dimensional solutions of the $(1 + 1)$ -dimensional GN model in higher dimensional models. This procedure is also adaptable to noninteger d , since the $(d - 1)$ -dimensional space perpendicular to the modulation can be treated in a way where d enters only as a parameter just as in the present study. This would enable us to observe how the degeneracy of the 1-dimensional solutions of the $1 + 1$ -dimensional GN model and homogeneous field configurations at $(\mu, T) = (\mu_c, 0)$ in $d = 2$ [32] develops for $1 < d < 2$.

The extension of the present analysis to nonzero temperature is under way. A nonzero temperature will likely not

change the conclusion about the (non)existence of the instability, since a nonzero temperature in all known occurrences disfavors an IP. However, it would reveal how the whole phase diagram evolves between the known results in integer spatial dimensions.

ACKNOWLEDGMENTS

I thank Adrian Koenigstein, Marc Winstel and Marc Wagner for their helpful comments on this manuscript and numerous, valuable discussions. Furthermore, I acknowledge fruitful, related discussions with Michael Buballa, Zohar Nussinov, Gergely Markó, Mike Ogilvie, Robert Pisarski, Fabian Rennecke, Stella Schindler and David Wagner. I acknowledge the support of the *Deutsche Forschungsgemeinschaft* (DFG, German Research Foundation) through the collaborative research center trans-regio CRC-TR 211 “Strong-interaction matter under extreme conditions”– project number 315477589 – TRR 211. I acknowledge the support of the *Helmholtz Graduate School for Hadron and Ion Research*. I acknowledge the support of the *Giersch Foundation*.

Appendix A: Derivation of the renormalized, homogeneous effective potential

In this Appendix, we outline the derivation of the renormalized, homogeneous effective potential by using a spatial momentum cutoff Λ to regularize the theory. A more detailed derivation and discussion can be found in Ref. [70]. The homogeneous effective potential was already investigated in Ref. [50], thus it is not original to this work. However, we need some of the results in the later derivation and hence it is instructive to also include the full derivation of the renormalized, effective potential here. Throughout this Appendix, we make regular use of the integral identities 3.194 from Ref. [71].

We start the derivation by calculating the integral l_0 that appears in the expression Eq. (7) and find that it evaluates to

$$\begin{aligned}
l_0 &= \frac{S_d}{(2\pi)^d} \int dp p^{d-1} [E - \Theta(\mu^2 - E^2)(E - |\mu|)] = \\
&= \frac{S_d}{(2\pi)^d} \frac{1}{d} \left[\Lambda^d |\bar{\sigma}| {}_2F_1\left(-\frac{1}{2}, \frac{d}{2}, \frac{d+2}{2}; -\left(\frac{\Lambda}{\bar{\sigma}}\right)^2\right) - \Theta(\bar{\mu}^2) |\bar{\sigma}|^{d+1} \left| \frac{\bar{\mu}}{\bar{\sigma}} \right|^d \left({}_2F_1\left(-\frac{1}{2}, \frac{d}{2}, \frac{d+2}{2}; -\frac{\bar{\mu}^2}{\bar{\sigma}^2}\right) - \left| \frac{\bar{\mu}}{\bar{\sigma}} \right| \right) \right] = \\
&= \frac{S_d}{(2\pi)^d} \frac{1}{2} \left[-\frac{|\bar{\sigma}|^{d+1} \Gamma\left(-\frac{d}{2} - \frac{1}{2}\right) \Gamma\left(\frac{d}{2} + 1\right)}{d\sqrt{\pi}} + \Lambda^d \left(\frac{2\Lambda}{d+1} + \frac{\bar{\sigma}^2}{(d-1)\Lambda} + \frac{\bar{\sigma}^4}{4(3-d)\Lambda^3} + \mathcal{O}(\Lambda^{-5}) \right) + \right. \\
&\quad \left. - \Theta(\bar{\mu}^2) |\bar{\sigma}|^{d+1} \left| \frac{\bar{\mu}}{\bar{\sigma}} \right|^d \left({}_2F_1\left(-\frac{1}{2}, \frac{d}{2}, \frac{d+2}{2}; -\frac{\bar{\mu}^2}{\bar{\sigma}^2}\right) - \left| \frac{\bar{\mu}}{\bar{\sigma}} \right| \right) \right], \tag{A1}
\end{aligned}$$

where $S_d = 2\pi^{\frac{d}{2}}/\Gamma\left(\frac{d}{2}\right)$ is the surface area of a d -dimensional unit sphere, $\bar{\mu}^2 = \mu^2 - \bar{\sigma}^2$ and we expanded the Λ dependent terms for $|\Lambda/\bar{\sigma}| \gg 1$ in the last step. ${}_2F_1$ denotes the Gaussian hypergeometric Function that can be represented via the integral

$${}_2F_1(\alpha, \beta; \gamma; z) = \frac{1}{B(\beta, \gamma - \beta)} \int_0^1 dt t^{\beta-1} (1-t)^{\gamma-\beta-1} (1-tz)^{-\alpha} \tag{A2}$$

with B being the Beta function.

In order to derive the renormalized, homogeneous effective potential, one needs to tune the coupling λ by imposing that the minimum of the renormalized, homogeneous effective potential in vacuum is at $\bar{\sigma} = \bar{\sigma}_0$. To do so, we employ the gap equation (8), where we need to calculate the integral l_1 . For the renormalization procedure, we would only need l_1 at $\mu = 0$ and finite $\bar{\sigma}$. However, we calculate it in its general μ and $\bar{\sigma}$ dependent form, since the same integral also appears in the bosonic two-point function that we need for the stability analysis. We find for the integral

$$\begin{aligned}
l_1(\bar{\sigma}^2, \mu, d) &= \int_{\Lambda} \frac{d^d p}{(2\pi)^d} \int_{-\infty}^{\infty} \frac{dp_0}{(2\pi)} \frac{1}{(p_0 - i\mu)^2 + E^2} = \frac{S_d}{(2\pi)^d} \int_0^{\Lambda} dp p^{d-1} \frac{1 - \Theta(\mu^2 - E^2)}{2E} = \\
&= \frac{S_d}{(2\pi)^d} \frac{1}{2d|\bar{\sigma}|} \left[\Lambda^d {}_2F_1\left(\frac{1}{2}, \frac{d}{2}, \frac{d+2}{2}; -\left(\frac{\Lambda}{\bar{\sigma}}\right)^2\right) - \Theta(\bar{\mu}^2) |\bar{\mu}|^d {}_2F_1\left(\frac{1}{2}, \frac{d}{2}, \frac{d+2}{2}; -\frac{\bar{\mu}^2}{\bar{\sigma}^2}\right) \right]. \tag{A3}
\end{aligned}$$

Using the vacuum part of this result and the gap equation (8), we tune the coupling to the appropriate value

$$\frac{1}{\lambda} = N_\gamma \frac{S_d}{(2\pi)^d} \frac{1}{2d\bar{\sigma}_0} \Lambda^d {}_2F_1 \left(\frac{1}{2}, \frac{d}{2}; \frac{d+2}{2}; -\left(\frac{\Lambda}{\bar{\sigma}_0}\right)^2 \right) = \quad (\text{A4})$$

$$= N_\gamma \frac{S_d}{(2\pi)^d} \frac{1}{2} \left[\frac{\bar{\sigma}_0^{d-1} \Gamma(\frac{d}{2} + 1) \Gamma(\frac{1}{2} - \frac{d}{2})}{d\sqrt{\pi}} + \Lambda^d \left(\frac{1}{(d-1)\Lambda} + \frac{\bar{\sigma}_0^2}{2(3-d)\Lambda^3} + \mathcal{O}(\Lambda^{-5}) \right) \right], \quad (\text{A5})$$

where we expanded the Λ dependent terms for $|\Lambda/\bar{\sigma}_0| \gg 1$. Inserting the expression for l_0 from Eq. (A1) and the tuned coupling into Eq. (7) yields the renormalized, homogeneous effective potential from Eq. (9), where a divergent, thermodynamically irrelevant constant term is neglected. We find for the symmetric limit $\bar{\sigma} \rightarrow 0$ that the renormalized effective potential is reduced to

$$\bar{U}_{\text{eff}}(\bar{\sigma} = 0, \mu, d) = \frac{N_\gamma}{2^d \pi^{\frac{d}{2}}} \frac{|\mu|^{d+1}}{\Gamma(\frac{d}{2}) d(d+1)}. \quad (\text{A6})$$

Appendix B: Derivation of the bosonic two-point function and the bosonic wave-function renormalization

In this Appendix, we outline the derivation of the bosonic two-point function and the wave-function renormalization. A more detailed derivation and discussion can be found in Ref. [70]. Throughout this Appendix, we make regular use of the integral identities 3.194 from Ref. [71].

The bosonic-two point function consists of a constant contribution $1/\lambda - N_\gamma l_1$, which is derived in Appendix A. Thus, we only need to calculate the integral L_2 that is given in Eq. (11). The first step is to get rid of any contributions that depend on the angle between the loop momentum \mathbf{p} and the external bosonic momentum \mathbf{q} . We can achieve this by applying a Feynman parametrization of the integral in Eq. (11) resulting in

$$\begin{aligned} l_2(\bar{\sigma}^2, \mu, q^2, d) &= N_\gamma \int_{-\infty}^{\infty} \frac{dp_0}{(2\pi)} \int \frac{d^d p}{(2\pi)^d} \int_0^1 dx \frac{1}{[(\mathbf{p} + \mathbf{q})^2 x + \Delta^2 x + (1-x)\mathbf{p}^2 + (1-x)\Delta^2]^2} = \\ &= N_\gamma \int_{-\infty}^{\infty} \frac{dp_0}{(2\pi)} \int \frac{d^d p}{(2\pi)^d} \int_0^1 dx \frac{1}{[p^2 + \Delta^2 + q^2 x(1-x)]^2} \end{aligned} \quad (\text{B1})$$

where we performed a shift of the integration variable $\mathbf{p} + \mathbf{q}x \rightarrow \mathbf{p}$ and $\Delta^2 = (p_0 - i\mu)^2 + \bar{\sigma}^2$. In this form we can easily carry out the integration over the temporal momenta and over the spatial momenta subsequently to obtain the form

$$\begin{aligned} l_2(\bar{\sigma}^2, \mu, q^2, d) &= N_\gamma \frac{S_d}{(2\pi)^d} \int_0^1 dx \int_0^\infty dp p^{d-1} \frac{1}{4\tilde{E}^3} \left[\Theta \left(\frac{\tilde{E}}{|\mu|} - 1 \right) - \frac{\tilde{E}}{|\mu|} \delta \left(\frac{\tilde{E}}{|\mu|} - 1 \right) \right] = \\ &= \frac{N_\gamma}{2^{d+1} \pi^{d/2} \Gamma(\frac{d}{2})} \int_0^1 dx \times \begin{cases} \frac{\tilde{\mu}^{d-3}}{(3-d)} {}_2F_1 \left(\frac{3}{2}, \frac{3-d}{2}; \frac{3-d}{2} + 1; -\frac{\tilde{\Delta}^2}{\tilde{\mu}^2} \right) - \frac{\tilde{\mu}^{d-2}}{|\mu|} & \text{if } \tilde{\mu}^2 > 0 \\ \frac{\tilde{\Delta}^{d-3}}{2} B \left(\frac{d}{2}, \frac{3-d}{2} \right) & \text{otherwise} \end{cases}, \end{aligned} \quad (\text{B2})$$

where $\tilde{E}^2 = \bar{\sigma}^2 + p^2 + q^2 x(1-x)$, $\tilde{\Delta}^2 = \bar{\sigma}^2 + q^2 x(1-x)$ and $\tilde{\mu}^2 = \mu^2 - \tilde{\Delta}^2$. Since only certain limits of $\bar{\sigma}^2$, μ^2 and q^2 allow to give a closed form expression of the integral over x , we simply evaluate the integral over x numerically. Inserting the result for l_2 (B2) and for $1/\lambda - l_1$ from Eqs. (A3) and (A5) into Eq. (10) yields the full two-point function from Eq. (12). The integral over x is trivial in the limit of $q \rightarrow 0$ for which we obtain for the two-point function the closed form

$$\begin{aligned} \Gamma^{(2)}(\bar{\sigma}^2, \mu, q^2 = 0, d) &= \frac{N_\gamma}{2^d \pi^{\frac{d}{2}} \Gamma(\frac{d}{2})} \left[\frac{\Gamma(\frac{1-d}{2}) \Gamma(\frac{d+2}{2})}{d\pi} (|\bar{\sigma}_0|^{d-1} - |\bar{\sigma}|^{d-1}) + \right. \\ &\quad \left. + \begin{cases} \frac{|\mu|^{d-1}}{(d-1)} & \text{if } \bar{\sigma} = 0, \mu \neq 0 \\ \frac{|\bar{\sigma}|^{d-1}}{d} \left| \frac{\tilde{\mu}}{\bar{\sigma}} \right|^d {}_2F_1 \left(\frac{1}{2}, \frac{d}{2}; \frac{d+2}{2}; -\frac{\tilde{\mu}^2}{\bar{\sigma}^2} \right) & \text{if } \bar{\sigma} \neq 0, \tilde{\mu}^2 > 0 \\ 0 & \text{otherwise} \end{cases} \right] + \end{aligned} \quad (\text{B3})$$

$$+|\bar{\sigma}|^{d-1} \times \left\{ \frac{1}{(3-d) \left| \frac{\bar{\mu}}{|\bar{\sigma}|} \right|} \left| \frac{\bar{\mu}}{|\bar{\sigma}|} \right|^{d-3} {}_2F_1 \left(\frac{3}{2}, \frac{3-d}{2}; \frac{3-d}{2} + 1; -\frac{\bar{\sigma}^2}{\bar{\mu}^2} \right) - \frac{\bar{\mu}^{d-2}}{|\mu|} \quad \text{if } \bar{\mu}^2 > 0 \right. \\ \left. \frac{1}{2} B \left(\frac{d}{2}, \frac{3-d}{2} \right) \quad \text{otherwise} \right\},$$

where $\bar{\mu}^2 = \mu^2 - \bar{\sigma}^2$.

The bosonic wave-function renormalization z is the curvature of the bosonic two-point function evaluated at $q = 0$. By differentiating L_2 twice with respect to q and evaluating it at $q = 0$, we find

$$z = \frac{1}{2} \frac{d^2 \Gamma^{(2)}(\bar{\sigma}, \mu, q^2, d)}{dq^2} \Big|_{q=0} = \frac{1}{4} N_\gamma \int_{-\infty}^{\infty} \frac{dp_0}{(2\pi)} \frac{S_d}{(2\pi)^d} \int_0^\infty dp p^{d-1} \left[\frac{2}{(E^2 + (p_0 - i\mu)^2)^2} - \frac{8\bar{\sigma}^2}{3(E^2 + (p_0 - i\mu)^2)^3} \right] \\ = \frac{1}{4} N_\gamma \frac{S_d}{(2\pi)^d} \int_0^\infty dp p^{d-1} \left\{ \frac{1}{2E^3} \left[\Theta \left(\frac{E^2}{\mu^2} - 1 \right) - \frac{E}{|\mu|} \delta \left(\frac{E}{|\mu|} - 1 \right) \right] + \right. \\ \left. - \frac{8\bar{\sigma}^2}{3} \frac{3}{16} \left[\frac{1}{E^5} \Theta(E^2 - \mu^2) - \frac{1}{E^4 |\mu|} \delta \left(\frac{E}{|\mu|} - 1 \right) + \frac{1}{3E^3 \mu^2} \delta' \left(\frac{E}{|\mu|} - 1 \right) \right] \right\}. \quad (\text{B4})$$

Carrying out the remaining integral over p results in the form given in Eq. (13).

-
- [1] M. Buballa and S. Carignano, Inhomogeneous chiral condensates, *Prog. Part. Nucl. Phys.* **81**, 39 (2015), [arxiv:1406.1367 \[hep-ph\]](#).
- [2] D. V. Deryagin, D. Yu. Grigoriev, and V. A. Rubakov, Standing wave ground state in high density, zero temperature QCD at large nc , *Int. J. Mod. Phys. A* **07**, 659 (1992).
- [3] D. Müller, M. Buballa, and J. Wambach, Dyson-Schwinger study of chiral density waves in QCD, *Physics Letters B* **727**, 240 (2013), [arxiv:1308.4303 \[hep-ph, physics:nucl-th\]](#).
- [4] T. F. Motta, J. Bernhardt, M. Buballa, and C. S. Fischer, Towards a Stability Analysis of Inhomogeneous Phases in QCD (2023), [arxiv:2306.09749 \[hep-ph, physics:nucl-th\]](#).
- [5] W.-j. Fu, J. M. Pawłowski, and F. Rennecke, The QCD phase structure at finite temperature and density, *Phys. Rev. D* **101**, 054032 (2020), [arxiv:1909.02991](#).
- [6] R. D. Pisarski, F. Rennecke, A. Tsvelik, and S. Valgushev, The Lifshitz Regime and its Experimental Signals, *Nuclear Physics A* **1005**, 121910 (2021), [arxiv:2005.00045](#).
- [7] R. D. Pisarski and F. Rennecke, Signatures of Moat Regimes in Heavy-Ion Collisions, *Phys. Rev. Lett.* **127**, 152302 (2021), [arxiv:2103.06890](#).
- [8] F. Rennecke and R. D. Pisarski, Moat Regimes in QCD and their Signatures in Heavy-Ion Collisions, *PoS CPOD2021*, 016 (2022), [arxiv:2110.02625](#).
- [9] F. Rennecke, R. D. Pisarski, and D. H. Rischke, Particle Interferometry in a Moat Regime (2023), [arxiv:2301.11484 \[hep-ph, physics:nucl-ex, physics:nucl-th\]](#).
- [10] M. A. Schindler, S. T. Schindler, L. Medina, and M. C. Ogilvie, Universality of Pattern Formation, *Phys. Rev. D* **102**, 114510 (2020).
- [11] M. A. Schindler, S. T. Schindler, and M. C. Ogilvie, \mathcal{PT} symmetry, pattern formation, and finite-density QCD (2021).
- [12] D. J. Gross and A. Neveu, Dynamical symmetry breaking in asymptotically free field theories, *Phys. Rev. D* **10**, 3235 (1974).
- [13] U. Wolff, The phase diagram of the infinite N Gross-Neveu model at finite temperature and chemical potential, *Phys. Lett.* **157B**, 303 (1985).
- [14] M. Thies and K. Urlichs, Revised phase diagram of the Gross-Neveu model, *Phys. Rev. D* **67**, 125015 (2003), [arxiv:hep-th/0302092](#).
- [15] O. Schnetz, M. Thies, and K. Urlichs, Phase diagram of the Gross-Neveu model: Exact results and condensed matter precursors, *Annals Phys.* **314**, 425 (2004), [arxiv:hep-th/0402014](#).
- [16] M. Thies, From relativistic quantum fields to condensed matter and back again: Updating the Gross-Neveu phase diagram, *J. Phys. A: Math. Gen.* **39**, 12707 (2006), [arxiv:hep-th/0601049](#).
- [17] A. Koenigstein, L. Pannullo, S. Rechenberger, M. Winstel, and M. J. Steil, Detecting inhomogeneous chiral condensation from the bosonic two-point function in the (1 + 1)-dimensional Gross-Neveu model in the mean-field approximation, *J. Phys. A: Math. Theor.* **55**, 375402 (2022), [arxiv:2112.07024 \[cond-mat, physics:hep-ph, physics:nucl-th\]](#).
- [18] D. Nickel and M. Buballa, Solitonic ground states in (color-) superconductivity, *Phys. Rev. D* **79**, 054009 (2009), [arxiv:0811.2400 \[cond-mat, physics:hep-ph, physics:nucl-th\]](#).
- [19] D. Nickel, Inhomogeneous phases in the Nambu-Jona-Lasino and quark-meson model, *Phys. Rev. D* **80**, 074025 (2009), [arxiv:0906.5295](#).

- [20] P. Adhikari and J. O. Andersen, Consistent regularization and renormalization in models with inhomogeneous phases, *Phys. Rev. D* **95**, 036009 (2017), [arxiv:1608.01097](#).
- [21] S. Carignano, D. Nickel, and M. Buballa, Influence of vector interaction and Polyakov loop dynamics on inhomogeneous chiral symmetry breaking phases, *Phys. Rev.* **82**, 054009 (2010), [arxiv:1007.1397 \[hep-ph\]](#).
- [22] S. Carignano, M. Schramm, and M. Buballa, Influence of vector interactions on the favored shape of inhomogeneous chiral condensates, *Phys. Rev.* **98**, 014033 (2018), [arxiv:1805.06203 \[hep-ph\]](#).
- [23] M. Buballa, L. Kurth, M. Wagner, and M. Winstel, Regulator dependence of inhomogeneous phases in the 2+1-dimensional Gross-Neveu model, *Phys. Rev. D* **103**, 034503 (2021), [arxiv:2012.09588](#).
- [24] F. Karsch, J. B. Kogut, and H. W. Wyld, The Gross-Neveu model at finite temperature and density, *Nucl. Phys. B* **280**, 289 (1987).
- [25] J. Lenz, L. Pannullo, M. Wagner, B. Wellegehausen, and A. Wipf, Inhomogeneous phases in the Gross-Neveu model in 1+1 dimensions at finite number of flavors, *Phys. Rev. D* **101**, 094512 (2020).
- [26] J. J. Lenz, L. Pannullo, M. Wagner, B. Wellegehausen, and A. Wipf, Baryons in the Gross-Neveu model in 1+1 dimensions at finite number of flavors, *Phys. Rev. D* **102**, 114501 (2020), [arxiv:2007.08382](#).
- [27] J. Stoll, N. Zorbach, A. Koenigstein, M. J. Steil, and S. Rechenberger, Bosonic fluctuations in the (1 + 1)-dimensional Gross-Neveu(-Yukawa) model at varying μ and T and finite N , [arXiv:2108.10616 \[cond-mat, physics:hep-ph, physics:nucl-th\]](#) (2021), [arxiv:2108.10616 \[cond-mat, physics:hep-ph, physics:nucl-th\]](#).
- [28] R. Ciccone, L. Di Pietro, and M. Serone, Inhomogeneous Phase of the Chiral Gross-Neveu Model, *Phys. Rev. Lett.* **129**, 071603 (2022).
- [29] J. J. Lenz, M. Mandl, and A. Wipf, Inhomogeneities in the 2-Flavor Chiral Gross-Neveu Model, *Phys. Rev. D* **105**, 034512 (2022), [arxiv:2109.05525 \[cond-mat, physics:hep-lat, physics:hep-th\]](#).
- [30] C. Nonaka and K. Horie, Inhomogeneous phases in the chiral Gross-Neveu model on the lattice, *PoS LATTICE2021*, 150 (2022).
- [31] A. Koenigstein, *Non-Perturbative Aspects of (Low-Dimensional) Quantum Field Theories*, Ph.D. thesis, Goethe University Frankfurt, Frankfurt am Main (2023).
- [32] K. Urlichs, *Baryons and Baryonic Matter in Four-Fermion Interaction Models*, Ph.D. thesis, Friedrich-Alexander-Universität Erlangen-Nürnberg (2007).
- [33] R. Narayanan, Phase diagram of the large N Gross-Neveu model in a finite periodic box, *Phys. Rev. D* **101**, 096001 (2020).
- [34] L. Pannullo and M. Winstel, [Absence of inhomogeneous chiral phases in 2+1-dimensional four-fermion and Yukawa models](#) (2023), [arxiv:2305.09444](#).
- [35] K. G. Klimenko, Phase Structure of Generalized Gross-Neveu Models, *Z. Phys. C* **37**, 457 (1988).
- [36] B. Rosenstein, B. J. Warr, and S. H. Park, Thermodynamics of (2+1)-dimensional Four Fermi Models, *Phys. Rev. D* **39**, 3088 (1989).
- [37] D. D. Scherer, J. Braun, and H. Gies, Many-flavor Phase Diagram of the (2+1)d Gross-Neveu Model at Finite Temperature, *J. Phys. A: Math. Theor.* **46**, 285002 (2013), [arxiv:1212.4624 \[cond-mat, physics:hep-lat, physics:hep-ph\]](#).
- [38] J. J. Lenz, M. Mandl, and A. Wipf, [The magnetized \(2+1\)-dimensional Gross-Neveu model at finite density](#) (2023), [arxiv:2304.14812 \[cond-mat, physics:hep-lat, physics:hep-th\]](#).
- [39] S. Hands, J. B. Kogut, C. G. Strouthos, and T. N. Tran, Fermi surface phenomena in the (2+1)D four-Fermi model, *Phys. Rev. D* **68**, 016005 (2003).
- [40] C. G. Strouthos, Mesons at finite baryon density in (2+1)d, *Prog. Theor. Phys. Suppl.* **153**, 69 (2004), [arxiv:hep-lat/0308021](#).
- [41] J. J. Lenz, M. Mandl, and A. Wipf, Magnetic catalysis in the (2+1)-dimensional Gross-Neveu model, *Phys. Rev. D* **107**, 094505 (2023), [arxiv:2302.05279 \[cond-mat, physics:hep-lat, physics:hep-th\]](#).
- [42] J. B. Kogut and C. G. Strouthos, Chiral symmetry restoration in the three-dimensional four-fermion model at non-zero temperature and density, *Phys. Rev. D* **63**, 054502 (2001), [arxiv:hep-lat/9904008](#).
- [43] S. Hands, A. Kocic, and J. Kogut, The Four-Fermi Model in Three Dimensions at Non-Zero Density and Temperature, *Nuclear Physics B* **390**, 355 (1993), [arxiv:hep-lat/9206024](#).
- [44] S. Hands, Four Fermion Models at Non-Zero Density, *Nuclear Physics A* **642**, c228 (1998), [arxiv:hep-lat/9806022](#).
- [45] T. L. Partyka and M. Sadzikowski, Phase diagram of the non-uniform chiral condensate in different regularization schemes at $T=0$, *J. Phys. G: Nucl. Part. Phys.* **36**, 025004 (2009), [arxiv:0811.4616 \[hep-ph\]](#).
- [46] H. Kohyama, D. Kimura, and T. Inagaki, Regularization dependence on phase diagram in Nambu–Jona-Lasinio model, *Nucl. Phys. B* **896**, 682 (2015).
- [47] L. Pannullo, M. Wagner, and M. Winstel, Inhomogeneous phases in the 3+1-dimensional Nambu–Jona-Lasinio model and their dependence on the regularization scheme, *PoS LATTICE2022*, 156 (2023).
- [48] A. E. B. Pasqualotto, R. L. S. Farias, W. R. Tavares, S. S. Avancini, and G. Krein, [Causality violation and the speed of sound of hot and dense quark matter in the Nambu–Jona-Lasinio model](#) (2023), [arxiv:2301.10721 \[hep-lat, physics:hep-ph, physics:hep-th, physics:nucl-th\]](#).
- [49] S. Carignano, M. Buballa, and B.-J. Schaefer, Inhomogeneous phases in the quark-meson model with vacuum fluctuations, *Phys. Rev. D* **90**, 014033 (2014), [arxiv:1404.0057](#).
- [50] T. Inagaki, T. Kouno, and T. Muta, Phase structure of four-fermion theories at finite temperature and chemical potential in arbitrary dimensions, *Int. J. Mod. Phys. A* **10**, 2241 (1995).
- [51] L. Pannullo, M. Wagner, and M. Winstel, Inhomogeneous phases in the chirally imbalanced 2+1-dimensional Gross-Neveu model and their absence in the continuum limit, *Symmetry* **14**, 265 (2022), [arxiv:2112.11183](#).
- [52] M. Buballa and S. Carignano, Inhomogeneous chiral phases away from the chiral limit, *Phys. Lett.* **B791**, 361 (2019),

- arxiv:1809.10066 [hep-ph].
- [53] A. Heinz, F. Giacosa, M. Wagner, and D. H. Rischke, Inhomogeneous condensation in effective models for QCD using the finite-mode approach, *Phys. Rev. D* **93**, 014007 (2016), arxiv:1508.06057 [hep-ph].
 - [54] P. de Forcrand and U. Wenger, New baryon matter in the lattice Gross-Neveu model, *PoS LAT2006*, 152 (2006), arxiv:hep-lat/0610117.
 - [55] M. Wagner, Fermions in the pseudoparticle approach, *Phys. Rev. D* **76**, 076002 (2007), arxiv:0704.3023.
 - [56] M. Buballa, S. Carignano, and L. Kurth, Inhomogeneous phases in the quark-meson model with explicit chiral-symmetry breaking, *Eur. Phys. J. Spec. Top.* **229**, 3371 (2020), arxiv:2006.02133.
 - [57] G. 't Hooft and M. Veltman, Regularization and renormalization of gauge fields, *Nuclear Physics B* **44**, 189 (1972).
 - [58] R. D. Pisarski, Chiral Symmetry Breaking in Three-Dimensional Electrodynamics, *Phys. Rev. D* **29**, 2423 (1984).
 - [59] H. Gies, L. Janssen, S. Rechenberger, and M. M. Scherer, Phase transition and critical behavior of d=3 chiral fermion models with left/right asymmetry, *Phys. Rev. D* **81**, 025009 (2010), arxiv:0910.0764.
 - [60] S. Hands, A. Kocic, and J. B. Kogut, Compositeness, anomalous dimensions and renormalizability in four Fermi theories, *Phys. Lett. B* **273**, 111 (1991).
 - [61] E. Nakano and T. Tatsumi, Chiral symmetry and density wave in quark matter, *Phys. Rev. D* **71**, 114006 (2005), arxiv:hep-ph/0411350.
 - [62] M. Sadzikowski and W. Broniowski, Non-uniform chiral phase in effective chiral quark models, *Physics Letters B* **488**, 63 (2000), arxiv:hep-ph/0003282.
 - [63] S. Carignano and M. Buballa, Inhomogeneous islands and continents in the Nambu–Jona-Lasinio model, *Acta Phys. Polon. Supp.* **5**, 641 (2012), arxiv:1111.4400.
 - [64] S. Carignano and M. Buballa, Two-dimensional chiral crystals in the NJL model, *Phys. Rev. D* **86**, 074018 (2012), arxiv:1203.5343 [hep-ph].
 - [65] P. Lakaschus, M. Buballa, and D. H. Rischke, Competition of inhomogeneous chiral phases and two-flavor color superconductivity in the NJL model, *Phys. Rev. D* **103**, 034030 (2021), arxiv:2012.07520.
 - [66] T. Inagaki, D. Kimura, and A. Kvinikhidze, π and σ mesons at finite temperature and density in the NJL model with dimensional regularization, *Phys. Rev. D* **77**, 116004 (2008), arxiv:0712.1336 [hep-ph].
 - [67] T. Inagaki, D. Kimura, H. Kohyama, and A. Kvinikhidze, Phase Diagram of Nambu–Jona-Lasinio Model with Dimensional Regularization, *Phys. Rev. D* **86**, 116013 (2012), arxiv:1202.5220.
 - [68] T. Fujihara, D. Kimura, T. Inagaki, and A. Kvinikhidze, High density quark matter in the NJL model with dimensional vs. cut-off regularization, *Phys. Rev. D* **79**, 096008 (2009), arxiv:0812.2821 [hep-ph].
 - [69] T. Fujihara, T. Inagaki, D. Kimura, and A. Kvinikhidze, Reconsideration of the 2-flavor NJL model with dimensional regularization at finite temperature and density, *Prog. Theor. Phys. Suppl.* **174**, 72 (2008), arxiv:0806.1331 [hep-ph].
 - [70] L. Pannullo, *Inhomogeneous Chiral Condensates in NJL-type Models on and off the Lattice*, Doctoral thesis, Goethe University Frankfurt (2023, in preparation).
 - [71] I. S. Gradshteyn, I. M. Ryzhik, and A. Jeffrey, *Table of Integrals, Series, and Products*, 7th ed. (Academic Press, Amsterdam ; Boston, 2007).